

DIGIMON: Diagnosis and Mitigation of Sampling Skew for Reinforcement Learning based Meta-Planner in Robot Navigation

Shiwei Feng, Xuan Chen, Zhiyuan Cheng, Zikang Xiong,
Yifei Gao, Siyuan Cheng, Sayali Kate and Xiangyu Zhang

Abstract—Robot navigation is increasingly crucial across applications like delivery services and warehouse management. The integration of Reinforcement Learning (RL) with classical planning has given rise to *meta-planners* that combine the adaptability of RL with the explainable decision-making of classical planners. However, the exploration capabilities of RL based meta-planners during training are often constrained by the capabilities of the underlying classical planners. This constraint can result in limited exploration, thereby leading to sampling skew issues. To address these issues, our paper introduces a novel framework, DIGIMON, which begins with *behavior-guided* diagnosis for exploration bottlenecks within the meta-planner and follows up with a mitigation strategy that conducts up-sampling from diagnosed bottleneck data. Our evaluation shows 13.5%+ improvement in navigation performance, greater robustness in out-of-distribution environments, and a 4× boost in training efficiency. DIGIMON is designed as a versatile, plug-and-play solution, allowing seamless integration into various RL-based meta-planners.

I. INTRODUCTION

Robot navigation is essential for applications like delivery services, hospital logistics, warehouse management, and library automation. Navigating cluttered environments remains a key challenge for achieving agile, efficient, and safe movement. Classical planners [1]–[4] address this by using specific cost functions and rules, which are difficult to generalize and often require expert manual tuning [5]–[8]. In contrast, learning-based approaches [9]–[15] offer adaptability but can suffer from instability and lack interpretability, leading to erratic behaviors that compromise safety and efficiency.

To overcome these limitations, recent studies introduced meta-planners [16], [17] that integrate RL with classical planning frameworks (see Fig. 1). RL-based meta-planners dynamically adjust the parameters of classical planners, combining RL’s adaptability with the explainable decision-making of classical methods for balanced robot navigation.

However, existing meta-planners suffer from sampling skew due to the integration of RL and classical planners. The exploration capabilities of RL are often limited by the classical planner’s inherent strategies. For instance, if the classical planner prefers conservative paths, the RL meta-planner may be unable to explore more aggressive or unconventional routes, resulting in sub-optimal performance. Previous approaches [18]–[22], such as adding noise to RL actions, do not address these specific integration challenges. Therefore, there is a crucial need for specialized methods to mitigate the biases introduced by combining RL meta-planners with classical planning.

*All authors are with Department of Computer Science, Purdue University.

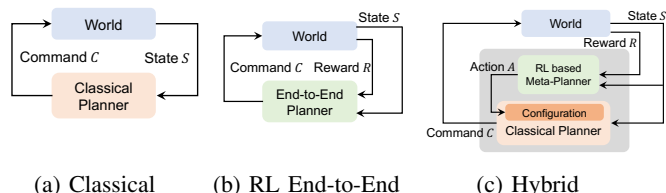


Fig. 1: Different Types of Planners. Note that the meta-planner is applied onto classical *local* planner f , not global trajectory planner.

In this paper, we propose DIGIMON, a diagnosis and mitigation framework addressing the limitations of RL meta-planners. DIGIMON starts with a *behavior-guided* diagnostic phase to identify exploration bottlenecks caused by classical planners. It then employs a novel up-sampling strategy to sample data from these bottleneck areas, providing RL meta-planner with a balanced replay buffer. This enhances RL exploration ability and mitigates sampling skew caused by classical planner’s preference. In summary, our contributions are:

- We identify and analyze the exploration bottlenecks and sampling skews arising from integrating RL with classical planning in meta-planners.
- We present DIGIMON, featuring a diagnostic phase to detect bottlenecks and a mitigation phase that uses data up-sampling to improve RL meta-planner training.
- DIGIMON achieves 13.5%+ improvement in navigation performance, greater robustness in out-of-distribution environments, and a 4× increase in training efficiency. Additionally, DIGIMON is a versatile, plug-and-play solution, compatible with various RL-based meta-planners.

II. BACKGROUND, NOTATIONS AND RELATED WORK

A. Motion Planning

Motion planning is used to determine a trajectory for a robot to move from a start position to a goal position while avoiding obstacles (as visualized in Fig. 2). It is worth noting that there are 2 major categories of planning algorithms: local trajectory planners (e.g. DWA [23], TEB [24]) and global path planners (e.g., Dijkstras [25], A* [26], RRT [27], [28]).

In this paper, we consider motion planning in navigation tasks and assume that the robot employs a classical *local* motion planner f . The local planner f can be tuned via a set of configurations (i.e., configurable parameters) $\theta \in \Theta$, where Θ denotes all possible values of planner configuration. While navigating in a physical world \mathcal{W} with obstacles, f tries to move the robot to a local goal $g_t \in \mathbb{R}^2$ (computed by the global planner). At each time step t , f receives sensor

observations o_t (e.g. lidar scans) to do collision avoidance, and then attempts to reach the local goal g_t in a fast and collision-free manner. The local planner f is responsible for computing the motion commands $u_t = f(o_t, g_t | \theta)$ (e.g., angular or linear velocity) at each time step to reach g_t .

B. Meta-Planner

Meta-Planner operates on top of the original planner f , adjusting its configuration θ . Fig. 1c shows that a hybrid planner with a meta-planner combines the explainability of classical planners with the adaptability of RL-based planners, enhancing performance. It has been applied across domains such as robot navigation [17], [29]–[31], autonomous driving [32], drone control [33], and robotic manipulation [34], [35].

There are two types of meta-planners: static and dynamic. Static meta-planners tune the configuration θ before deployment, while dynamic meta-planners adjust it in real-time.

Static. Bayesian optimization is often used to auto-tune parameters for black-box systems [36]–[38]. By iteratively updating its model of the objective function, it efficiently explores the parameter space, tuning planning parameters for better performance.

Dynamic. Dynamic meta-planners adjust parameters on-the-fly for different scenarios [15], [16], [39], [40]. For example, [15] learns a library of parameter sets and switches based on context, while [16] uses reinforcement learning to optimize parameter policies over decision sequences.

C. RL as Meta-Planner

While existing works [41], [42] combine RL with rule-based classical planning to enhance *global* path planning, our paper focuses on integrating RL with a *local* planner.

We formulate the navigation problem with a meta-planner as a Markov Decision Process (MDP) \mathcal{M} , i.e., a tuple $(\mathcal{S}, \mathcal{A}, \mathcal{T}, \gamma, \mathcal{R})$. $\mathcal{T} : \mathcal{S} \times \mathcal{A} \rightarrow \mathcal{S}$ is the state transition function, $\mathcal{R} : \mathcal{S} \times \mathcal{A} \rightarrow \mathcal{R}$ is the reward function, and γ is the discount factor. At each time step t , the RL agent takes the current state $s_t \in \mathcal{S}$ as input and outputs an action $a_t \in \mathcal{A}$. Then the environment will transit to the next state $s_{t+1} \sim \mathcal{T}(\cdot | s_t, a_t)$ and the agent will receive a reward $r_t = \mathcal{R}(s_t, a_t)$. The overall objective of RL agent is to learn a policy $\pi : \mathcal{S} \rightarrow \mathcal{A}$ that can be used to select actions that maximize the expected cumulative reward over time, i.e. $J = \mathbb{E}_{(s_t, a_t) \sim \pi} [\sum_{t=0}^{\infty} \gamma^t r_t]$.

Within the MDP, we optimize a meta-planner policy that interacts with a composite environment consisting of the navigation world \mathcal{W} (filled with obstacles) and a configurable motion planner f parameterized by θ and receiving sensory inputs o . The state space, action space, reward function, and termination conditions are defined as follows:

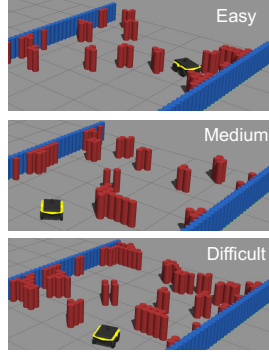


Fig. 2: Maps of various difficulty levels.

State space. Following [16], we assume a local goal g is always reachable and acts as a waypoint on a global path. The direction to g , $\phi \in [-\pi, \pi]$, relative to the robot’s orientation, provides directional information. Thus, the state is $s_t = (o_t, \phi_t, \theta_{t-1})$, where o_t are sensory inputs, ϕ_t the angle to g , and θ_{t-1} the previous planner configuration.

Action space. The agent’s action $a_t = \pi(s_t)$ updates the planner’s parameters θ_t . Executing a_t applies θ_t to planner f , moving the robot and transitioning to the next state s_{t+1} .

Reward. The agent receives an immediate reward r_t inversely related to its distance to g . An episode ends when a maximum time T is reached or a termination condition is triggered, with the final reward penalizing timeouts and collisions.

The goal of the RL agent within the meta-planner is to learn a policy π that can select a planner parameter θ_t for f to achieve optimal navigation performance. The objective can be formulated as:

$$\max_{\pi} J^{\pi} = \mathbb{E}_{s_0, \theta_t \sim \pi(s_t), s_{t+1} \sim \mathcal{T}(s_t, \theta_t)} \left[\sum_{t=0}^{\infty} \gamma^t r_t \right]. \quad (1)$$

D. Prioritized Experience Replay

Prioritized Experience Replay [43] improves RL by assigning higher probabilities to more informative experiences in the replay buffer, enhancing learning efficiency. It selects samples that significantly contribute to the agent’s progress. In contrast, our approach focuses on improving data collection quality by reducing sampling bias and promoting better exploration, resulting in a more informative replay buffer. Together, these methods complement each other to advance RL efficiency.

E. Roadmap Analysis

Existing roadmap analysis [44], [45] often relies on static geometric properties to address challenges like narrow passages, using concepts such as visibility and lookout. While these studies provide valuable insights, they do not fully capture the dynamic execution status resulting from a robot’s interaction with environment. Our approach aims to enhance performance by leveraging robot behavior during dynamic execution. By analyzing the robot’s behaviors as it operates, we identify high-resistance areas that may not be apparent through static analysis alone. This behavior-guided method allows us to adaptively improve planning and navigation, leading to better performance than static geometric analysis.

III. SAMPLING SKEW OF EXISTING METHODS

APPLR [16], the state-of-the-art dynamic meta-planner, exhibits a sampling skew that can lead to inefficiencies and limit performance improvements. In this section, we discuss the sampling skew, key insights, and related technical challenges.

Meta-Planner Training. Fig. 3 shows 2D projections of the *difficult* map from Fig. 2, where the robot navigates obstacles from the start (left) to the goal (right) without collisions and within a time limit. The meta-planner adjusts planner’s configurations, i.e. actions $a_t = \pi(s_t)$, at a fixed frequency (e.g., 1 Hz) in response to environmental changes, and we record the robot’s positions for reward calculation and policy training.

Fig. 3a shows the early-stage challenges with a randomly initialized policy, where the robot often gets stuck (Area

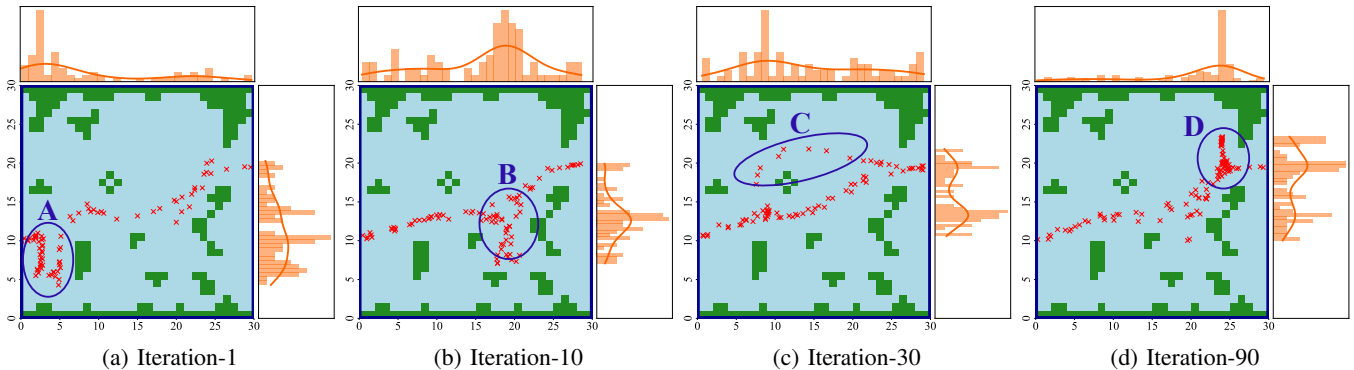


Fig. 3: Sampling skew in existing RL-based Meta-Planner. For convenient visualization, we show 2D projections of the difficult map from Fig. 2 and omit the robot body. The start position is on the left of the map and the goal is on the right. Red cross markers are the robot trajectories at each timestamp. On top and right of the maps are the frequency distribution of robot positions x and y .

A). Over time (Fig. 3b), the policy improves, avoiding early obstacles but still struggling with tight spaces. As training progresses (Fig. 3c), the robot reduces getting stuck but takes inefficient detours (Area C), leading to timeout. Further training (Fig. 3d) improves navigation, but the robot still faces difficulties passing through narrow gates (Area D).

Sampling Skew Phenomenon. From training iterations in Fig. 3, sampling skew can be summarized by 3 observations: *Observation I: Challenging scenarios require more sampling.* In difficult situations like dead corners (Fig. 3b), detours (Fig. 3c), and narrow gates (Figures 3a, 3d), the classical planner’s limitations and insufficient sampling of the meta-planner often cause delays, timeouts, or collisions. These critical *hard-to-pass* areas require significantly more sampling to improve navigation efficiency and safety.

Observation II: Challenging scenarios have impact on subsequent scenarios. *Hard-to-pass* areas make the following scenarios (i.e., *hard-to-reach*) more difficult to access. This is reflected in the robot’s position distribution, showing higher frequency near *hard-to-pass* areas (e.g., Area A in Fig. 3a and Area B in Fig. 3b) and lower frequency in subsequent regions.

Observation III: Challenging scenarios tend to be under-fitted. Certain challenging scenarios remain under-fitted, risking mission success due to two key factors. For instance, Area D initially remains *hard-to-reach* (Fig. 3a-3c) and is not effectively trained. As training progresses (Fig. 3d), Area D becomes *hard-to-pass*, as the robot reaches it smoothly but takes around 20 steps (about 20 seconds) per trajectory. This lengthy process limits efficient training within a fixed budget, making it difficult to fully train Area D.

Challenges. A simple solution to mitigate sampling skew is to focus on training the meta-planner more in under-fitted areas, but there is no automatic way to identify these regions. Analyzing static maps alone is insufficient (e.g., detecting narrow parts or sharp turns), as this only considers static information and ignores how the robot dynamically executes and interacts with its environment.

Our key insight is that *hard-to-reach* areas stem from preceding *hard-to-pass* areas. If there are no *hard-to-pass* areas, the robot can easily and safely reach its goal. Therefore, our robot *behavior-guided* method focuses on: (1) increasing

sampling in *hard-to-pass* areas based on Observations I and II, and (2) reducing the time needed to initiate such sampling, aligning with Observation III. In Section IV, we describe how we identify these areas to address issues in meta-planner.

IV. DESIGN OF DIGIMON

We introduce DIGIMON, consisting of two components: *diagnosis* (Section IV-B) and *mitigation* (Section IV-C) of sampling skew phenomenon, as discussed in Section III.

A. Overview

Alg. 1 illustrates the integration of DIGIMON within the meta-planner policy training pipeline. Components enhanced by DIGIMON are highlighted in blue, indicating the modifications to the standard meta-planner policy. The remaining parts abstract the conventional components of a reinforcement learning training pipeline.

To better quantitatively pinpoint the *hard-to-pass* areas discussed in Section III, we develop Alg. 2 and define the concept *high-resistance area* (\mathcal{H}), composed of specific poses termed *high-resistance points*. Intuitively, *high-resistance* refers to the observation of abrupt *behavioral* changes by the robot at these points, suggesting that these areas pose significant uncertainty to the robot’s behavior.

B. Sampling Skew Diagnosis

High-Resistance Point Identification. Alg. 2 identifies high-resistance areas \mathcal{H} within robot’s navigation environment. By processing pose trajectories \mathcal{P} and a threshold η , it outputs \mathcal{H} , i.e. poses where the robot exhibits significant behavioral changes, indicating challenging regions for the planner.

The algorithm begins by accepting a set of pose trajectories \mathcal{P} . For each trajectory in \mathcal{P} , the algorithm checks if the trajectory successfully reaches the mission goal, filtering out any mission-failure trajectories (in Line 5 of Alg. 2). For trajectories that reach the mission goal, the algorithm examines each triplet of consecutive poses (p_i, p_{i+1}, p_{i+2}) within the trajectory. The poses are characterized by their position x, y and orientation w .

In Line 11 of Alg. 2, the differences in x and y coordinates between consecutive robot poses are used to calculate *trajectory orientations*, notated as $\rho_i = \arctan(\Delta y_i / \Delta x_i)$ and

Algorithm 1 DIGIMON for Enhancing RL-based Meta-Planner Training

1: **Input:** Initial meta-planner policy network π , high-resistance area \mathcal{H} , environment $\mathcal{E} = f \times \mathcal{W}$ for π (where f is classical planner and \mathcal{W} is physical map).
2: **Constants:** Robot’s initial position INIT_POSE, threshold λ for sampling initial pose from \mathcal{H} , policy training iteration N , trajectory collection number K , policy update number L .
3: **Output:** The converged meta-planner policy network π^* .
4: Set $\mathcal{D} = \mathcal{P} = \mathcal{H} = \emptyset$. \triangleright transition buffer \mathcal{D} , pose buffer \mathcal{P}
5: **for** iteration $n = 0, \dots, N$ **do**
6: **for** $k = 0, \dots, K$ **do**
7: Initialize state s_0 by resetting \mathcal{E} .
8: Set the robot’s initial pose $p_0 = \text{INIT_POSE}$.
9: Set transition buffer $\mathcal{D}_k = \emptyset$, robot pose buffer $\mathcal{P}_k = \emptyset$.
10: **if** $\text{getRandom}(0,1) < \lambda$ and $\mathcal{H} \neq \emptyset$ **then**
11: $p_0 \leftarrow \text{getRandom}(\mathcal{H})$
12: Set $\tilde{s} = [s_0]$ and $\tilde{p} = [p_0]$.
13: **for** $t = 0, \dots, T$ **do**
14: Run π in \mathcal{E} , take action $a_t = \pi(s_t)$.
15: Obtain reward r_t , state s_{t+1} and pose p_{t+1} .
16: $\tilde{s} \leftarrow \tilde{s}.\text{append}(s_{t+1})$, $\tilde{p} \leftarrow \tilde{p}.\text{append}(p_{t+1})$.
17: **if** π gets done signal from \mathcal{E} **then**,
18: $\mathcal{D}_k \leftarrow \mathcal{D}_k \cup \{\tilde{s}\}$, $\mathcal{P}_k \leftarrow \mathcal{P}_k \cup \{\tilde{p}\}$.
19: Update \mathcal{D} using \mathcal{D}_k . \triangleright This step is algorithm-specific
20: Update \mathcal{H} : $\mathcal{H} \leftarrow \text{getHRArea}(\mathcal{P}_k)$. \triangleright Refer to Alg. 2.
21: **for** $\ell = 0, \dots, L$ **do**
22: $\mathcal{B} \leftarrow \text{getMiniBatch}(\mathcal{D})$ \triangleright Random mini-batch
23: Update policy π using \mathcal{B} . \triangleright Algorithm-specific
24: Return the final meta-planner policy π^* .

$\rho_{i+1} = \arctan(\Delta y_{i+1}/\Delta x_{i+1})$. Then variation of trajectory orientations $\Delta\rho_i = \rho_{i+1} - \rho_i$ is then normalized to the range $[-\pi, \pi]$ (in Line 12 of Alg. 2). If the absolute value $|\Delta\rho_i|$ exceeds the threshold η , the corresponding pose p_i is identified as a high-resistance point and added to the set \mathcal{H} . Finally, the algorithm returns the set \mathcal{H} , representing the high-resistance area. The key intuition behind Alg. 2 is to capture regions where the meta planner shows high uncertainty in challenging scenarios, indicated by a high variance in the trajectory.

Note that there are two technical aspects that merit particular attention: ❶ Alg. 2 employs variations in trajectory orientations $\Delta\rho$ rather than robot orientations Δw as the metric for comparison against the threshold η . This design effectively captures behaviors such as back-and-forth movements, where the robot’s orientation may remain relatively unchanged and thus cannot be detected by Δw . However, these movements are also clear indicators of challenges faced by the planner. ❷ Alg. 2 strategically excludes failure trajectories. This exclusion ensures that any points of high resistance can ultimately reach the goal. Allowing the robot to persist in areas that are excessively challenging would cause the planner to become indefinitely stuck, thereby introducing noise into the training of the meta-planner. This process allows for the identification of challenging areas where the robot experiences significant difficulties, enabling targeted interventions to improve the planner’s performance in these regions.

C. Sampling Skew Mitigation

High-Resistance Area Up-sampling. In Lines 10-11 of Alg. 1, the process of high-resistance area up-sampling is implemented to enhance the robustness and adaptability of the meta-planner during training. This algorithm leverages threshold $\lambda \in [0, 1]$ to determine whether to sample the

Algorithm 2 High-Resistance Area Identification getHRArea

1: **Input:** Pose trajectory set \mathcal{P} , threshold η for high-resistance identification.
2: **Output:** High-resistance area \mathcal{H} .
3: Initialize $\mathcal{H} = \emptyset$.
4: **for** each \tilde{p} in \mathcal{P} **do**
5: **if** \tilde{p} reaches the mission goal **then**
6: $\triangleright p$ is a 3-dim vector: position x, y and orientation w
7: **for** each (p_i, p_{i+1}, p_{i+2}) in \tilde{p} **do**
8: $(x_k, y_k, w_k) \leftarrow p_k, k = \{i, i+1, i+2\}$, .
9: $\Delta x_i, \Delta x_{i+1} \leftarrow x_{i+1} - x_i, x_{i+2} - x_{i+1}$.
10: $\Delta y_i, \Delta y_{i+1} \leftarrow y_{i+1} - y_i, y_{i+2} - y_{i+1}$.
11: $\rho_i, \rho_{i+1} \leftarrow \arctan\left(\frac{\Delta y_i}{\Delta x_i}\right), \arctan\left(\frac{\Delta y_{i+1}}{\Delta x_{i+1}}\right)$
12: $\Delta\rho_i \leftarrow \rho_{i+1} - \rho_i$.
13: $\Delta\rho_i \leftarrow (\Delta\rho_i \bmod 2\pi) - \pi$. \triangleright Normalization
14: **if** $|\Delta\rho_i| > \eta$ **then** $\mathcal{H} \leftarrow \mathcal{H} \cup \{p_i\}$
15: Return the high-resistance area \mathcal{H} .

robot’s initial position from the set of high-resistance areas \mathcal{H} . It ensures that the meta-planner frequently encounters and learns to navigate through high-resistance regions, thereby improving its ability to handle challenging scenarios. By balancing this targeted exploration with a general exploration of the environment, the meta-planner will train more efficiently and effectively in high-resistance areas. Additionally, \mathcal{H} is updated iteratively in Line 20 of Alg. 1, ensuring that the set of high-resistance areas remains relevant and accurately reflects the current sampling challenges. This iterative update is crucial for maintaining the effectiveness of the up-sampling strategy. Overall, the up-sampling of high-resistance areas is critical for the meta-planner’s training as it enhances the planner’s robustness, promotes better generalization to new environments, and addresses sampling skew.

V. EVALUATION

A. Experiment Setup

Simulation & Planners. Following existing works [15], [16], we implement DIGIMON using the widely-used Gazebo [46] simulator with a ClearPath Jackal differential drive ground robot as a robot model. Due to space limit, we leave the details of the classical planner and the meta-planner that DIGIMON builds upon for evaluation to Appendix VII.

Baselines & Dataset. We compare DIGIMON with two widely used classical planners (DWA [23] and DWA-Fast [47]), one representative static meta-planner, BayesOpt [36] and one SOTA dynamic RL-based meta-planner APPLR [16]. We choose the same dataset as APPLR, namely BARN [48] dataset, as it includes various maps for robot navigation inside the Gazebo simulator and it has different difficulty levels’ map (i.e., Easy, Medium, and Difficult) to evaluate. This allows for a convenient evaluation of various planners’ performance across these varied settings.

Metrics. We evaluate navigation systems using five metrics: ❶ Actual Traveling Time (ATT): Time (in seconds) to complete successful missions. ❷ Mission Success Rate (SR): Percentage of missions completed (i.e., reaching the goal without collisions and within the time budget.). ❸ Collision Rate (CR): Percentage of missions failed due to collisions with obstacles. ❹ Timeout Rate (TR): Percentage of missions

TABLE I: Navigation performance of DIGIMON and baseline methods under **Same-Env** setup.

Metric ⇒ Method ↓	Easy					Medium					Difficult				
	NS ↑	ATT ↓	SR ↑	CR ↓	TR ↓	NS ↑	ATT ↓	SR ↑	CR ↓	TR ↓	NS ↑	ATT ↓	SR ↑	CR ↓	TR ↓
DWA	20.72	30.01	97.65	1.18	1.18	16.91	33.35	90.59	2.35	7.06	10.61	30.99	53.75	16.25	30.00
DWA-Fast	25.44	23.60	76.47	23.53	0.00	16.30	30.68	64.71	23.53	11.76	12.43	27.40	50.00	18.75	31.25
BayesOpt	17.88	48.09	74.00	10.00	16.00	15.61	21.84	49.02	21.57	29.41	5.94	58.37	43.75	6.25	50.00
APPLR	20.19	28.48	70.59	13.24	16.18	21.36	26.36	85.29	7.35	7.35	12.83	33.59	57.81	4.69	37.50
Ours	35.03	13.45	80.88	11.76	7.35	23.23	21.62	76.74	17.65	5.88	14.56	27.81	60.94	18.75	20.31

NS: Navigation Score. ATT: Actual Traveling Time. SR: Success Rate. CR: Collision Rate. TR: Timeout Rate.

TABLE II: Navigation performance of DIGIMON and baselines under **Cross-Env** and **Cross-Level** setups. The column names represent the test environment levels: All (across all three levels), Easy, Medium and Difficult.

Training Env.	Metric ⇒ Method ↓	All					Easy					Medium					Difficult				
		NS ↑	ATT ↓	SR ↑	CR ↓	TR ↓	NS ↑	ATT ↓	SR ↑	CR ↓	TR ↓	NS ↑	ATT ↓	SR ↑	CR ↓	TR ↓	NS ↑	ATT ↓	SR ↑	CR ↓	TR ↓
Easy	BayesOpt	12.67	44.58	72.00	10.00	18.00	18.33	37.00	88.24	0.00	11.76	12.68	45.81	76.47	17.65	5.88	6.65	56.79	50.00	12.50	37.50
	APPLR	10.46	37.91	47.60	19.60	32.80	20.04	29.82	71.76	12.94	15.29	7.06	44.63	44.71	17.65	37.65	3.90	49.80	25.00	28.75	46.25
	Ours	20.43	19.04	58.40	15.20	26.40	35.32	14.08	82.35	11.76	5.88	15.26	22.16	50.59	22.35	27.06	10.10	25.48	41.25	11.25	47.50
Medium	BayesOpt	19.74	17.68	52.00	16.00	32.00	35.18	10.78	76.47	5.88	17.65	13.38	25.33	41.18	29.41	29.41	10.09	23.72	37.50	12.50	50.00
	APPLR	21.85	25.39	77.60	11.60	11.80	31.43	20.71	90.59	9.41	0.00	21.49	26.89	84.71	7.06	8.24	12.06	31.02	56.25	18.75	25.00
	Ours	24.39	22.22	75.20	13.60	11.20	37.14	15.66	92.94	7.06	0.00	22.61	22.40	75.29	18.82	5.88	12.73	33.47	56.25	15.00	28.75
Difficult	BayesOpt	8.72	52.23	52.00	10.00	38.00	11.32	43.11	58.82	5.88	35.29	8.87	54.66	52.94	5.88	41.18	5.81	62.13	43.75	18.75	37.50
	APPLR	22.56	25.21	76.00	8.40	15.60	34.51	18.93	92.94	5.88	1.18	19.65	26.69	75.29	12.94	11.76	12.97	33.74	58.75	6.25	35.00
	Ours	24.61	22.54	79.60	12.00	8.40	36.30	17.90	96.47	3.53	0.00	22.16	24.53	80.00	12.94	7.06	14.78	27.56	61.25	20.00	18.75

NS: Navigation Score. ATT: Actual Traveling Time. SR: Success Rate. CR: Collision Rate. TR: Timeout Rate.

where the robot failed to reach the goal within the time limit.

⑤ **Navigation Score (NS)**: A comprehensive performance metric from BARN Challenge [49], calculated as follows:

$$NS_i = \mathbb{I}(\text{Success}) \times \frac{OT_i}{\text{clip}(\text{ATT}_i, 2OT_i, 8OT_i)} \quad (2)$$

Here, OT_i represents the optimal time (computed using Dijkstra algorithm [50] in advance), and $\text{clip}(\text{ATT}_i, 2OT_i, 8OT_i)$ ensures that the actual traveling time is constrained within twice and eight times the optimal time. $\mathbb{I}(\text{Success})$ is an indicator function that denotes whether the current navigation mission is successful, consistent with the definition of SR. Higher values of NS and SR indicate better performance, while lower values of ATT, CR, and TR indicate better performance.

Comparison Setup. We introduce 3 evaluation setups: (1) **Same-Env**: The meta-planner is trained and tested in the same environment set with predefined but different start positions to avoid overfitting. (2) **Cross-Env**: The meta-planner is trained and tested at the same difficulty level but in different environments. (3) **Cross-Level**: The meta-planner is trained on one difficulty level but tested on a different difficulty level.

B. Same-environment Performance

We evaluate DIGIMON and four baselines under the **Same-Env** setup. DWA, DWA-Fast, and BayesOpt are static planners, so we directly implement their fixed configurations from the training environment and test them on the same environments with random starting positions. For APPLR and DIGIMON, we train the meta-planner policy on the training set and deploy it on the test environments.

Table I shows that DIGIMON consistently achieves the highest NS score across all difficulty levels, demonstrating its ability to identify and improve performance in underrepresented scenarios. While DWA performs better on SR and CR in easy and medium environments, DIGIMON excels in the comprehensive NS metric. DWA’s conservative design prioritizes safety over time efficiency, leading to longer navigation times, as seen in reduced ATT and lower NS scores, making it less practical for navigation tasks. Since NS is a widely-used metric [15], [16], DIGIMON’s higher NS score effectively demonstrates its superiority over both static planners and the SOTA dynamic meta-planner.

C. Cross-environment & Cross-level Performance

In this section, we compare DIGIMON and selected baselines under the **Cross-Env** and **Cross-Level** setup, as shown in the diagonal sub-tables in Table II. Under the **Cross-Env** setup, DIGIMON consistently achieves the highest NS score across all three environments, indicating its effectiveness in identifying and addressing underrepresented scenarios to enhance planner performance. For the **Cross-Level** experiments, DIGIMON excels in generalization by achieving the highest NS scores when the trained meta-planner is tested across different environmental difficulty levels. This demonstrates DIGIMON’s robustness and capability to maintain navigation efficacy in new and varying conditions. Additionally, when meta-planners trained in difficult environments are applied to easier ones, DIGIMON outperforms even those baselines specifically trained for simpler environments, while this trend is not observed in the baseline methods. This result suggests that the meta-planners trained by our method can learn

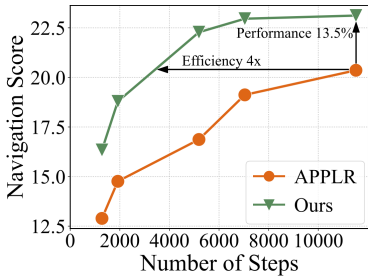


Fig. 4: Navigation score (NS) of different checkpoints.

TABLE III: Performance of DIGIMON on PPO-based meta-planner.

	PPO + APPLR	PPO + Ours
NS \uparrow	17.58	20.61
ATT \downarrow	24.69	22.07
SR \uparrow	55.56	65.28
CR \downarrow	26.39	15.28
TR \downarrow	18.06	19.44

TABLE IV: Performance of DIGIMON w/ and w/o failure filtering.

	w/o Filtering	w/ Filtering
NS \uparrow	22.22	23.23
ATT \downarrow	19.60	21.62
SR \uparrow	70.59	76.47
CR \downarrow	22.06	17.65
TR \downarrow	7.35	5.88

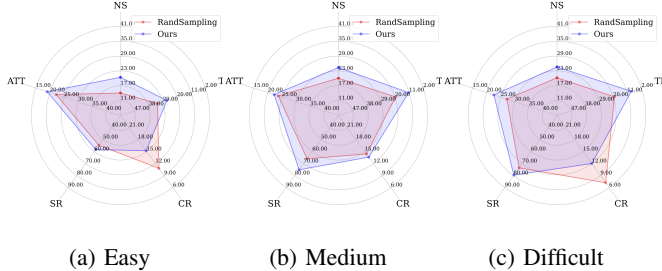


Fig. 5: Comparison of RandomSampling and DIGIMON. The meta-planners are trained on three different difficulty levels and tested across all levels.

more sophisticated and adaptable configurations, enabling DIGIMON to excel in environments that are less challenging.

D. Diagnosis Effectiveness

To better understand why our diagnosis and mitigation strategy is effective, we introduce a variant called Random-Sampling (RS). Unlike DIGIMON, which identifies high-resistance areas with Alg. 2, RS indiscriminately samples from all locations reached by the robot during training without strategic guidance, while all other designs remain consistent with DIGIMON. Results in Fig. 5 show that DIGIMON significantly outperforms RS, with higher NS scores in all environments. The reasons are two-fold. First, RS fails to expose the robot to challenging, hard-to-reach scenarios, limiting effective training in these high-resistance areas, which is a crucial aspect for satisfactory navigation performance. Second, as shown in Fig. 2, medium and hard environments have more complicated maps with many hard-to-reach scenarios and obstacles than the easy level. Random sampling in such environments often leads to the robot encountering “dead-corner” scenarios – areas that are hard to exit, leading to extended, unrewarding training trajectories. Such trajectories will destabilize the training of the RL policy in the meta-planner and degrade navigation performance. This analysis verifies the necessity of our high-resistance area up-sampling step in DIGIMON. By strategically selecting those hard-to-reach areas, we enhance the robot’s ability to perform well across a variety of navigational scenarios. Appendix VIII shows more results in the comparison between RS and DIGIMON.

E. Efficiency

In this section, we evaluate the performance of different meta-planner policy checkpoints during training under the

Cross-Env setup when DIGIMON is applied in a medium-level environment. Fig. 4 shows the average NS metric when those checkpoints are evaluated in testing environments. DIGIMON consistently outperforms APPLR, achieving higher navigation scores at all training stages with the same training steps. Furthermore, APPLR requires over *four times* training steps to achieve comparable performance of DIGIMON, and our method ultimately outperforms APPLR by 13.5%. These results demonstrate that our method significantly enhances the training efficiency of the RL policy within the meta-planner and improves the overall navigation performance of the robot. Besides NS, we also show more metrics of different meta-planner checkpoints during training (in Fig. 11 in Appendix).

F. Plug-and-Play Applicability on Other RL Algorithm

In Sections V-B and V-C, we have demonstrated that DIGIMON enhances navigation performance when paired with the off-policy algorithm TD3 [51] based meta-planner in APPLR. To further validate the versatility of DIGIMON, we extended it to another SOTA on-policy RL algorithm, Proximal Policy Optimization (PPO) [52]. For a fair comparison, we replace the TD3 training algorithm in APPLR with PPO. Results are shown in Table III. We can observe that DIGIMON outperforms baseline methods when applied to PPO, where four out of five metrics get significantly improved, and a negligible drop in timeout rate. This indicates that compared to APPLR, our diagnostic method is robust across various training algorithms and not limited to a specific algorithm.

G. Other Experiments

Ablation study. We conduct the ablation study to justify the importance of key components in DIGIMON and the sensitivity test against the key hyper-parameters. Details can be found in Appendix IX-B.

VI. CONCLUSION

In this paper, we identify and analyze the challenges of integrating RL with classical planning in meta-planners. While this integration enhances adaptability and explainability, it introduces sampling skew due to the conservative nature of classical planners, limiting the RL meta-planners’ exploration and performance in complex environments.

To address these issues, we propose DIGIMON, a diagnostic and mitigation framework for RL-based meta-planners.

DIGIMON analyzes robot behaviors, identifies exploration bottlenecks and applies a targeted up-sampling strategy to balance the sampling data, enabling more effective learning and exploration. Our experiments demonstrate that DIGIMON improves navigation performance by 13.5%+, enhances robustness in unseen environments, and quadruples training efficiency.

Limitations. Although DIGIMON greatly boosts efficiency, further optimization of training duration is possible. The current pipeline depends on executing the classical planner to collect data, meaning increased complexity of the classical planner can raise training costs. Additionally, DIGIMON is specifically designed for navigation tasks and may not apply to manipulation tasks, which we leave for future work.

REFERENCES

- [1] J. A. Abdulsahab and D. J. Kadhim, "Robot path planning in unknown environments with multi-objectives using an improved coot optimization algorithm." *International Journal of Intelligent Engineering & Systems*, 2022.
- [2] T. Asano, T. Asano, L. Guibas, J. Hershberger, and H. Imai, "Visibility-polygon search and euclidean shortest paths," in *26th annual symposium on foundations of computer science*. IEEE.
- [3] J. F. Canny, "A voronoi method for the piano-movers problem," *Proceedings. 1985 IEEE International Conference on Robotics and Automation*, 1985.
- [4] M. Elbhanhawi and M. Simic, "Sampling-based robot motion planning: A review," *IEEE Access*, 2014.
- [5] S. Campbell, N. O'Mahony, A. Carvalho, L. Krpalkova, D. Riordan, and J. Walsh, "Path planning techniques for mobile robots a review," in *ICMRE*, 2020.
- [6] F. A. Raheem, S. M. Raafat, and S. M. Mahdi, "Robot path-planning research applications in static and dynamic environments," *Earth Systems Protection and Sustainability: Volume 1*, 2022.
- [7] K. Zheng, "Ros navigation tuning guide," *Robot Operating System (ROS) The Complete Reference (Volume 6)*, pp. 197–226, 2021.
- [8] S. Feng, Y. Ye, Q. Shi, Z. Cheng, X. Xu, S. Cheng, H. Choi, and X. Zhang, "Rocas: Root cause analysis of autonomous driving accidents via cyber-physical co-mutation," 2024. [Online]. Available: <https://arxiv.org/abs/2409.07774>
- [9] M. Pfeiffer, M. Schaeuble, J. Nieto, R. Siegwart, and C. Cadena, "From perception to decision: A data-driven approach to end-to-end motion planning for autonomous ground robots," in *ICRA*, 2017.
- [10] W. Gao, D. Hsu, W. S. Lee, S. Shen, and K. Subramanian, "Intention-net: Integrating planning and deep learning for goal-directed autonomous navigation," in *Conference on robot learning*, 2017.
- [11] H.-T. L. Chiang, A. Faust, M. Fiser, and A. Francis, "Learning navigation behaviors end-to-end with autolr," *IEEE Robotics and Automation Letters*, 2019.
- [12] X. Xiao, B. Liu, G. Warnell, and P. Stone, "Toward agile maneuvers in highly constrained spaces: Learning from hallucination," *IEEE Robotics and Automation Letters*, 2021.
- [13] B. Liu, X. Xiao, and P. Stone, "A lifelong learning approach to mobile robot navigation," *IEEE Robotics and Automation Letters*, 2021.
- [14] X. Xiao, B. Liu, and P. Stone, "Agile robot navigation through hallucinated learning and sober deployment," in *ICRA*, 2021.
- [15] X. Xiao, B. Liu, G. Warnell, J. Fink, and P. Stone, "Appld: Adaptive planner parameter learning from demonstration," *IEEE Robotics and Automation Letters*, 2020.
- [16] Z. Xu, G. Dhamankar, A. Nair, X. Xiao, G. Warnell, B. Liu, Z. Wang, and P. Stone, "Applr: Adaptive planner parameter learning from reinforcement," in *ICRA*, 2021.
- [17] X. Xiao, B. Liu, G. Warnell, and P. Stone, "Motion planning and control for mobile robot navigation using machine learning: a survey," *Autonomous Robots*, 2022.
- [18] P. Swazinna, S. Udfluft, and T. Runkler, "Overcoming model bias for robust offline deep reinforcement learning," *Engineering Applications of Artificial Intelligence*, 2021.
- [19] W. Shen, R. Zheng, W. Zhan, J. Zhao, S. Dou, T. Gui, Q. Zhang, and X. Huang, "Loose lips sink ships: Mitigating length bias in reinforcement learning from human feedback," *arXiv preprint arXiv:2310.05199*, 2023.
- [20] M. S. Mark, A. Sharma, F. Tajwar, R. Rafailov, S. Levine, and C. Finn, "Offline RL for online RL: Decoupled policy learning for mitigating exploration bias," 2024.
- [21] A. L. Strehl and M. L. Littman, "A theoretical analysis of model-based interval estimation," *Proceedings of the 22nd international conference on Machine learning*, 2005.
- [22] E. Nikishin, M. Schwarzer, P. D'Oro, P.-L. Bacon, and A. Courville, "The primacy bias in deep reinforcement learning," in *International Conference on Machine Learning*, 2022.
- [23] D. Fox, W. Burgard, and S. Thrun, "The dynamic window approach to collision avoidance," *IEEE Robotics & Automation Magazine*, 1997.
- [24] "Ted local planner," https://wiki.ros.org/teb_local_planner.
- [25] E. DIJKSTRA, "A note on two problems in connexion with graphs," *Numerische Mathematik*, vol. 1, pp. 269–271, 1959. [Online]. Available: <http://eudml.org/doc/131436>
- [26] P. E. Hart, N. J. Nilsson, and B. Raphael, "A formal basis for the heuristic determination of minimum cost paths," *IEEE Transactions on Systems Science and Cybernetics*, vol. 4, no. 2, pp. 100–107, 1968.
- [27] S. M. LaValle, "Rapidly-exploring random trees : a new tool for path planning," *The annual research report*, 1998. [Online]. Available: <https://api.semanticscholar.org/CorpusID:14744621>
- [28] S. M. LaValle and J. J. Kuffner Jr, "Randomized kinodynamic planning," *The international journal of robotics research*, vol. 20, no. 5, pp. 378–400, 2001.
- [29] D. Fridovich-Keil, S. L. Herbert, J. F. Fisac, S. Deglurkar, and C. J. Tomlin, "Planning, fast and slow: A framework for adaptive real-time safe trajectory planning," in *ICRA*, 2018.
- [30] S. Siva, M. Wigness, J. Rogers, and H. Zhang, "Robot adaptation to unstructured terrains by joint representation and apprenticeship learning," in *Robotics: Science and Systems*, 2019.
- [31] A. Pokle, R. Martín-Martín, P. Goebel, V. Chow, H. M. Ewald, J. Yang, Z. Wang, A. Sadeghian, D. Sadigh, S. Savarese *et al.*, "Deep local trajectory replanning and control for robot navigation," in *ICRA*, 2019.
- [32] S. Jiang, Z. Xiong, W. Lin, Y. Cao, Z. Xia, J. Miao, and Q. Luo, "An efficient framework for reliable and personalized motion planner in autonomous driving," *IEEE Robotics and Automation Letters*, p. 8, 2022.
- [33] A. Loquercio, A. Saviolo, and D. Scaramuzza, "Autotune: Controller tuning for high-speed flight," *IEEE Robotics and Automation Letters*, 2022.
- [34] M. Moll, C. Chamzas, Z. K. Kingston, and L. E. Kavraki, "Hyperplan: A framework for motion planning algorithm selection and parameter optimization," *IROS*, 2021.
- [35] Y. Jia, J. Xu, D. Jayaraman, and S. Song, "Dynamic grasping with a learned meta-controller," *arXiv preprint arXiv:2302.08463*, 2023.
- [36] J. Snoek, H. Larochelle, and R. P. Adams, "Practical bayesian optimization of machine learning algorithms," *NeurIPS*, 2012.
- [37] B. Shahriari, K. Swersky, Z. Wang, R. P. Adams, and N. De Freitas, "Taking the human out of the loop: A review of bayesian optimization," *Proceedings of the IEEE*, 2015.
- [38] P. I. Frazier, "A tutorial on bayesian optimization," *arXiv preprint arXiv:1807.02811*, 2018.
- [39] X. Xiao, J. Biswas, and P. Stone, "Learning inverse kinodynamics for accurate high-speed off-road navigation on unstructured terrain," *IEEE Robotics and Automation Letters*, 2021.
- [40] A. Binch, G. P. Das, J. Pulido Fentanes, and M. Hanheide, "Context dependant iterative parameter optimisation for robust robot navigation," in *ICRA*, 2020.
- [41] S. Gu, G. Chen, L. Zhang, J. Hou, Y. Hu, and A. Knoll, "Constrained reinforcement learning for vehicle motion planning with topological reachability analysis," *Robotics*, vol. 11, p. 81, 2022. [Online]. Available: <https://api.semanticscholar.org/CorpusID:251651462>
- [42] C. Gehring, M. Asai, R. Chitnis, T. Silver, L. Kaelbling, S. Sohrabi, and M. Katz, "Reinforcement learning for classical planning: Viewing heuristics as dense reward generators," in *Proceedings of the International Conference on Automated Planning and Scheduling*, vol. 32, 2022, pp. 588–596.
- [43] T. Schaul, J. Quan, I. Antonoglou, and D. Silver, "Prioritized experience replay," in *4th International Conference on Learning Representations, ICLR 2016, San Juan, Puerto Rico, May 2-4, 2016, Conference Track Proceedings*, Y. Bengio and Y. LeCun, Eds., 2016. [Online]. Available: <http://arxiv.org/abs/1511.05952>
- [44] L. Kavraki, M. Kolountzakis, and J.-C. Latombe, "Analysis of probabilistic roadmaps for path planning," *IEEE Transactions on Robotics and Automation*, vol. 14, no. 1, pp. 166–171, 1998.

- [45] D. Hsu, J.-C. Latombe, and H. Kurniawati, “On the probabilistic foundations of probabilistic roadmap planning,” *Int. J. Rob. Res.*, vol. 25, no. 7, p. 627–643, jul 2006. [Online]. Available: <https://doi.org/10.1177/0278364906067174>
- [46] N. Koenig and A. Howard, “Design and use paradigms for gazebo, an open-source multi-robot simulator,” in *IROS*, 2004.
- [47] Z. Xu, “Dwa-fast,” https://github.com/Daffan/the-barn-challenge/tree/fast_dwa, 2022.
- [48] D. Perille, A. Truong, X. Xiao, and P. Stone, “Benchmarking metric ground navigation,” in *SSRR*, 2020.
- [49] “Barn challenge competition,” https://cs.gmu.edu/~xiao/Research/BARN_Challenge/BARN_Challenge23.html, 2023.
- [50] E. W. Dijkstra, “A note on two problems in connexion with graphs,” in *Edsger Wýbe Dijkstra: His Life, Work, and Legacy*, 2022.
- [51] S. Fujimoto, H. Hoof, and D. Meger, “Addressing function approximation error in actor-critic methods,” in *ICML*, 2018.
- [52] J. Schulman, F. Wolski, P. Dhariwal, A. Radford, and O. Klimov, “Proximal policy optimization algorithms,” *arXiv preprint arXiv:1707.06347*, 2017.

APPENDIX

VII. EXPERIMENT SETUP

We run experiments on Ubuntu 20.04, with Intel i9-13900K, 64 GB RAM and Nvidia GPU RTX 2080. The robot is equipped with a 720-dimensional planar laser scanner with a 270° field of view, which provides our sensory input o_t . We pre-process the LiDAR scans by capping the maximum range to 2m. The onboard Robot Operating System (ROS) move_base navigation stack (our underlying classical motion planner f) uses Dijkstra’s algorithm [50] to plan a global path and runs DWA [23] as the local classical planner to follow the global path.

The meta-planner policy π is trained to update the planning configurations θ of the classical planner. We maintain the same settings as APPLR, utilizing the DWA classical planner and the same action space θ , including `max_vel_x`, `max_vel_theta`, `vx_samples`, `vtheta_samples`, `occdist_scale`, `pdist_scale`, `gdist_scale`, and `inflation_radius`.¹ We use the ROS dynamic reconfigure client to dynamically change planner parameters. The global goal α is assigned manually, while θ_0 is the default set of parameters provided by the robot manufacturer.² Table V shows the details of each configuration of the meta-planner.

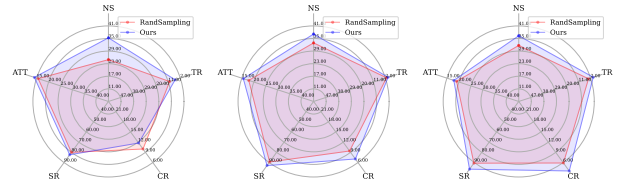
VIII. DIAGNOSIS EFFECTIVENESS

In this section, we delve deeper into the comparative analysis between RandomSampling and DIGIMON by applying both methods across environments of varying complexity: Easy, Medium, and Difficult. We conducted separate experiments for each difficulty level, which allowed for detailed and direct comparisons. The results of these experiments are represented in Figures 6, 7, and 8.

Consistent with the observations discussed in Section V-D, our DIGIMON continues to outperform RandomSampling in overall navigation performance. This superiority is quantified by a higher Navigation Score (NS), indicating DIGIMON’s effectiveness in handling complex navigation tasks. This

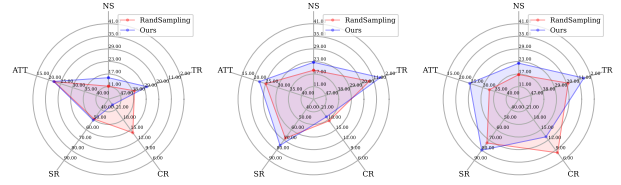
¹https://wiki.ros.org/dwa_local_planner

²http://wiki.ros.org/costmap_2d



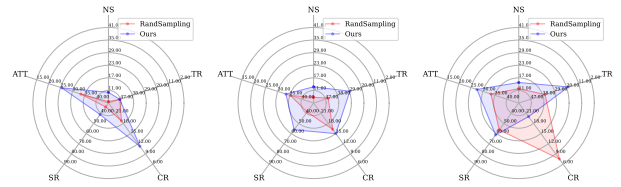
(a) Train on Easy (b) Train on Medium (c) Train on Difficult

Fig. 6: Test on Easy Level



(a) Train on Easy (b) Train on Medium (c) Train on Difficult

Fig. 7: Test on Medium Level



(a) Train on Easy (b) Train on Medium (c) Train on Difficult

Fig. 8: Test on Difficult Level

comparison not only highlights the strengths of DIGIMON but also contributes to a better understanding of its operational dynamics across different environmental settings.

IX. ADDITIONAL EXPERIMENTS

A. More Results of Efficiency Comparison

In Figure 11, we present additional metrics for various meta-planner checkpoints during training, including average traveling time, reward, and success rate. It clearly shows that DIGIMON outperforms APPLR across all three metrics. Notably, DIGIMON requires fewer training steps to achieve shorter traveling times, highlighting the method’s efficiency. Similarly, within the same amount of training steps, DIGIMON can also achieve a higher average reward and success rate. All of these three metrics robustly demonstrate that DIGIMON can achieve superior efficacy compared to the SOTA baseline APPLR.

B. Ablation Study

Sensitivity. We conduct ablation studies to evaluate the sensitivity of DIGIMON against various crucial hyper-parameters: (1) high-resistance area sampling threshold λ in Algorithm 1 and (2) high-resistance point identification threshold η in Algorithm 2.

Failure Trajectory Filtering. We evaluate the necessity of our failure trajectory filtering in DIGIMON and its advantages

Configuration	Min	Max	Meaning
max_vel_x	0.1	2.0	m/s. Maximum threshold for linear velocity.
max_vel_theta	0.314	3.14	rad/s. The absolute value of the maximum rotational velocity for the robot.
vx_samples	4	12	The number of samples to use when exploring the x velocity space.
vtheta_samples	8	40	The number of samples to use when exploring the theta velocity space
path_distance_bias	0.1	0.5	The weight for how much the robot should stay close to the path it was given.
goal_distance_bias	0.1	2	The weight for how much the robot should attempt to reach its local goal.
inflation_radius	0.1	0.6	Controls how far away the zero cost point is from obstacle.

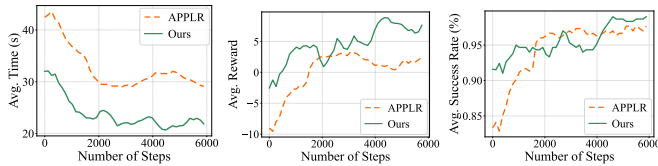
TABLE V: Action Space of Meta-Planner Policy π .

TABLE VI: Navigation performance under different high-resistance area up-sampling ratios λ .

Ratio λ	NS \uparrow	ATT \downarrow	SR \uparrow	CR \downarrow	TR \downarrow
0.2	9.63	27.01	38.75	25.00	36.25
0.4	13.33	31.63	57.50	12.50	30.00
0.6	11.18	38.38	55.00	13.75	31.25
0.8	11.59	27.04	42.50	17.50	40.00

TABLE VII: Navigation performance under different trajectory vector change thresholds η .

Threshold η ($^\circ$)	NS \uparrow	ATT \downarrow	SR \uparrow	CR \downarrow	TR \downarrow
50	15.19	26.89	50.59	18.82	30.59
70	18.92	26.78	65.20	14.80	20.00
90	22.61	22.40	75.29	18.82	5.88
110	18.22	28.93	74.12	15.29	10.59
130	17.45	23.70	57.65	14.12	28.24



(a) Average Time (a) Average Reward (a) Average Success Rate

Fig. 11: Average time, reward, and success rate of DIGIMON and APPLR for different checkpoints during training.

for improving navigation performance. The results are shown in Table IV. We observe that without the failure filtering trajectory mechanism, three out of five metrics deteriorate significantly, particularly the collision rate and success rate, which are critical to the robot’s safety. In contrast, without failure filtering, the NS and ATT metrics show only marginal improvements. This indicates that filtering out failure trajectories can substantially enhance overall navigation performance in terms of safety and task completion rate while not sacrificing total travel time.

High-resistance Area Up-sampling Ratio λ . We then study the influence of λ in Alg. 1 on the navigation performance. Table VI shows that $\lambda = 0.4$ yields the best performance for the navigation system. Varying λ introduces fluctuations across various metrics, while all within a 10% range. This demonstrates the necessity of fine-tuning the high-resistance area up-sampling ratio λ to balance the proportion of difficult trajectories within the total training set. If λ is set too high, the training set will contain too many challenging trajectories, complicating the meta-planner’s ability to understand the complete map and complete the task. If λ is set too low, it will revert to the original training method, hindering the meta-planner’s ability to learn from

those under-fitted trajectories.

In Table VII, we show the performance metrics of DIGIMON over different threshold angles. While there are some improvements in certain metrics (e.g., NS and CR) at higher threshold angles, the performance data clearly converges around 90° as the optimal threshold for overall system performance. This peak suggests at 90° , the system achieves a balance between speed, efficiency, and safety, highlighting a degree of robustness and adaptability. Similar to the high-resistance area up-sampling ratio λ , the threshold angle should also be carefully tuned to enable the best performance. Thus, we set $\lambda = 0.4$ and $\eta = 90$ for all other experiments.

X. POTENTIAL SOCIAL IMPACTS

The development and deployment of DIGIMON, aimed at enhancing the performance of meta-planner policy in robotic navigation, promises significant positive social benefits. By enabling robots to navigate more effectively and reliably, our tool can greatly facilitate the integration of robotics into our daily life. For example, in healthcare settings, more efficient navigation can enable robots to deliver medication, assist in surgeries, or provide companionship with greater precision and safety. In homes, robots equipped with advanced navigation capabilities can assist individuals with disabilities, offering them greater independence and quality of life. Furthermore, in disaster response situations, robots that can navigate challenging terrains could save lives by reaching areas that are inaccessible to humans. Overall, by improving the reliability and functionality of meta-planners in robotic navigation systems, DIGIMON has the potential to make significant contributions to society, improving safety, accessibility, and efficiency in numerous critical areas.